Journal of Operation and Automation in Power Engineering

vol. 13, no. Special Issue, Dec. 2025, Pages: 44-53

http://joape.uma.ac.ir

Research Paper

Load–Frequency Control of a Restructured Multi-Area Power System with DFIG-Based Wind Integration Using Coordinated AVR–PSS–FACTS and Optimized PID Controllers

Isayev Fakhriddin [1, *], *Olim Tursunov* [2], *Khamidova Suluv Yangiboevna* [3], *Mirzokhid Ernazarov* [4], *Otabek Mirzaev* [5], *Fakhriddin Khurramovich Karimov* [6], and *Khudoyarov Anvar Nazirjonovich* [7]

[1]*Scientific Research Center "Scientific Foundations and Problems of the Development of the Economy of Uzbekistan", under Tashkent State University of Economics, Tashkent, Uzbekistan.*
[2]*Alfraganus University, House 2a, Yuqori Qoraqamish Street, Tashkent, 100190, Uzbekistan.*
[3]*Termez State University of Engineering and Agrotechnologies, Termez , Uzbekistan.*
[4]*Termez University of Economics and Service, Termez, Uzbekistan.*
[5]*Urgench State University named after Abu Rayhan Biruni, Urgench, Uzbekistan.*
[6]*Tashkent State University of Economics, Tashkent, Uzbekistan.*
[7]*Urgench State University named after Abu Rayhan Biruni, Urgench, Uzbekistan.*

Abstract— *This study investigates load–frequency control (LFC) in a restructured multi-area power system with significant renewable energy integration, where increased stochasticity and reduced inertia intensify frequency deviations. A coordinated control strategy combining automatic voltage regulator (AVR), power system stabilizer (PSS), thyristor-controlled phase shifter (TCPS), and optimized PID controllers is proposed to improve dynamic performance under competitive market conditions. Metaheuristic optimization techniques are employed to tune controller parameters for robustness across operating scenarios, including high renewable penetration and contractual power transactions. Simulation results demonstrate that the coordinated scheme substantially reduces overshoot, settling time, and frequency oscillations compared with conventional control approaches. The findings confirm that integrating auxiliary damping devices with optimized LFC significantly enhances frequency stability and resilience in modern deregulated power systems.*

Keywords—Restructured power system, doubly-fed induction generator, optimization algorithms, particle swarm optimization, iperialist competitive algorithm.

1. INTRODUCTION

In restructured power systems, generation companies create a competitive environment for energy trading by dynamically adjusting electricity selling prices [1]. These price fluctuations influence both the supply and demand of electricity, subsequently impacting grid stability [2]. Furthermore, the increasing penetration of renewable energy sources poses new challenges for Load Frequency Control (LFC) system operation [3]. Renewable sources, such as wind turbines and photovoltaic systems, exhibit inherent variability and unpredictability, leading to power and frequency oscillations within the network [4]. These oscillations, coupled with real-time electricity price variations, can degrade power quality and even trigger instability in the power system. Therefore, accurate and effective frequency control is essential in such environments [5, 6].

In contemporary power networks, inadequate frequency control can lead to imbalances between generation and load, potentially resulting in system-wide blackouts during critical conditions [7]. In multi-area systems, each area comprises a set of generators and loads, and maintaining a uniform frequency across the entire area is crucial [8]. A key approach to managing this challenge is the utilization of Automatic Generation Control (AGC), which measures the Area Control Error (ACE) to detect real power imbalances and adjusts generator output to maintain frequency stability [9]. This paper examines frequency control strategies within a restructured environment, considering the dynamics of the electricity market and the integration of renewable energy sources. We propose intelligent optimization algorithms to enhance the performance of the frequency control system.

Examining the impact of the competitive electricity market environment is of particular importance, as understanding these effects can lead to the discovery of novel approaches for optimizing frequency control in multi-area systems [10]. Several studies in reputable scientific sources have analyzed the impact of restructuring on AGC [11, 12]. Among renewable energy sources, wind energy is of significant importance due to its notable advantages over other renewable options [13]. Therefore, efficient management of wind energy conversion systems is essential for improving network performance [14]. One of the fundamental challenges in operating wind turbines is their fixed-speed operation,

Received: 27 Nov. 2025
Revised: 27 Dec. 2025
Accepted: 29 Dec. 2025
*Corresponding author:
E-mail: f.isayev@tsue.uz (I. Fakhriddin)
DOI: 10.22098/joape.2025.18913.2466

which prevents the turbine from consistently operating at its optimal operating point. This leads to a decrease in the energy captured from the wind. However, the use of variable-speed wind turbines, equipped with Doubly-Fed Induction Generators (DFIGs), allows for adjusting the optimal operating point at any wind speed. In this scenario, as the wind speed changes, the optimal operating point of the turbine changes, and the rotor speed is adjusted accordingly [15]. Therefore, examining the contribution of wind energy extraction to frequency control, especially under distributed generation and competitive market conditions, is essential [16]. To improve power system stability and reduce frequency fluctuations, the implementation of a Power System Stabilizer (PSS) [17] in the Automatic Voltage Regulator (AVR) loop has been proposed [18]. Furthermore, the use of controllers based on Thyristor Controlled Phase Shifters (TCPS) [19] in interconnected power systems has a positive impact on reducing frequency fluctuations, as confirmed by previous studies [20].

Control methods include classical control (such as PID) [21], modern control (such as state-space methods) [22], optimal control (such as LQR) [23], adaptive control [24], robust control [25], fuzzy control [26], and intelligent control (such as neural networks and machine learning algorithms) [27]. Optimization techniques play a crucial role in enhancing control performance across various engineering domains, and in this study they are employed to obtain the most effective PID parameters for improving multi-area frequency stability [27]. In interconnected power systems, various disturbances can compromise the stability of each area. To address these challenges, flexible control strategies are crucial. A common approach involves using a PID controller within the LFC framework to dampen oscillations and maintain power balance. Optimal parameter tuning of the PID controller is vital for its effective operation, and various optimization algorithms, including GA [28], PSO [29], and the relatively new and powerful ICA [30], are employed for this purpose. While the performance of restructured power systems has been explored in previous studies [31], the impact of renewable energy sources and volatile electricity markets has often been overlooked. In particular, many studies assume a fixed electricity price, neglecting the dynamic nature of energy procurement [32]. Although the role of variable-speed wind turbines in frequency regulation has been investigated [6, 20], this has not been done within a restructured market framework. This research addresses these limitations by investigating the integrated effect of a restructured power system, a volatile electricity market, and the presence of renewable energy sources on frequency control, aiming to provide effective solutions for enhancing stability and mitigating system oscillations. Recent studies have also explored advanced control approaches for improving power-system frequency stability under uncertainty. For example, the authors in [33] proposed an enhanced adaptive control strategy capable of handling disturbances and structural variations in interconnected power systems. Similarly, [34] introduced an intelligent control framework combining learning-based methods with dynamic system modeling to improve transient and frequency stability in multi-area grids. These contributions illustrate the growing trend toward integrating adaptive, intelligent, and optimization-based controllers to overcome limitations of classical AGC designs. In this context, the present study contributes by developing a coordinated AVR–PSS–TCPS architecture combined with optimized PID controllers, offering a practical yet effective solution to enhance system stability under restructured and renewable-integrated operating conditions. Existing studies on AGC in deregulated environments generally focus on either the impact of contract-based power exchanges or the design of optimized controllers for frequency regulation, but rarely address their interaction with renewable variability. Works on RES-integrated AGC primarily examine wind or solar penetration without incorporating realistic market-driven power shifts, and only a limited number consider detailed DFIG inertial dynamics. Similarly, studies employing AVR–PSS coordination or FACTS devices such as TCPS typically evaluate damping and tie-line control independently of pricing mechanisms and contractual disturbances. Furthermore, optimization-based PID tuning has been widely investigated, yet most contributions benchmark algorithms in simplified or isolated settings that do not include coordinated voltage regulation, flow control, and renewable uncertainty simultaneously. To our knowledge, no prior research has integrated dynamic electricity-market behavior, inertia-aware DFIG modeling, AVR–PSS–TCPS coordination, and multi-algorithm PID tuning within a unified LFC framework. This absence of a comprehensive comparative analysis under realistic restructured scenarios defines the primary gap addressed in this study.

Unlike conventional AGC studies that examine deregulated operation, renewable penetration, or supplementary damping controls in isolation, the present work integrates these elements into a single, coherent methodological framework. First, the model incorporates market-driven, time-varying contractual exchanges among distribution and generation companies, enabling explicit simulation of frequency disturbances induced by real-time electricity price updates. Second, inertia-aware DFIG dynamics are embedded into the multi-area system to capture the influence of wind penetration on primary frequency support. Third, AVR–PSS coordination and a TCPS device are incorporated directly into the AGC loop to enhance both local damping and inter-area oscillation suppression. Finally, the PID-based LFC controller is tuned using three population-based optimization algorithms—ICA, GA, and PSO—under a unified ITAE performance index, allowing systematic comparison within the same operational framework. The combined treatment of market dynamics, renewable generation behavior, and coordinated damping and flow-control mechanisms represents the central methodological advancement of this study and differentiates it from earlier works in restructured power system frequency control. With the restructuring of the electricity industry and the creation of competitive markets, electricity prices fluctuate in real-time based on supply and demand. These price fluctuations directly impact the amount of electricity purchased by distribution companies, and consequently, the balance between generation and consumption. Furthermore, with the increasing use of renewable energy sources, especially wind power plants, new challenges in frequency stability have emerged. The output power of these sources depends on environmental conditions, and their real-time changes cause oscillations in the power system frequency. In this situation, effective frequency control has become an essential necessity to maintain network stability and prevent potential disruptions.

In this study, the term restructured power system refers to the organizational unbundling of generation companies (GENCOs), distribution companies (DISCOs), and transmission operators, as commonly implemented in deregulated electricity sectors. This restructuring does not change the physical dynamics of the system, but modifies the contractual framework under which power is generated and exchanged. The term market in this context refers to the price-driven adjustment of contracts between GENCOs and DISCOs. These contract variations lead to time-varying scheduled power transfers, which act as external disturbances to the multi-area AGC loop. Thus, although market behavior itself is not the subject of analysis, market-induced variations directly affect frequency stability and tie-line oscillations. The present study therefore focuses on the stability implications of such disturbances, rather than on market economics, and develops a coordinated control approach for mitigating their impact.

Despite substantial progress in AGC research, existing studies typically examine market restructuring effects, renewable generation uncertainty, and optimization-based controller tuning as separate issues. The interaction among these elements—particularly how price-driven contractual shifts, inertia-deficient DFIG-based wind plants, and coordinated damping devices jointly influence multi-area frequency dynamics—remains insufficiently explored. Previous works also lack a unified framework that incorporates both inter-

area oscillation damping (AVR–PSS and TCPS) and optimized LFC tuning under market-induced disturbances. This gap motivates the present study, which integrates these aspects into a single coherent methodology to assess their combined impact on system stability. This research investigates the frequency control in a dynamic, competitive electricity market where the amount of energy purchased from generation companies changes intermittently. To cope with fluctuations caused by price variations and the integration of renewable energy sources, a hybrid control system consisting of a PID controller, FACTS devices, an AVR, and a PSS is employed. In addition, the controller parameters are tuned using several optimization algorithms, and their effectiveness in improving system frequency stability is evaluated.

2. METHOD

2.1. Modeling of AVR with PSS and dynamic model for TCPS compensator

The AVR plays a critical role in maintaining voltage stability by regulating the excitation of synchronous generators. The PSS enhances the AVR's functionality by providing supplementary control signals that damp electromechanical oscillations, thereby improving transient stability. Furthermore, the TCPS compensator provides dynamic control of power flow across transmission lines, offering an additional degree of freedom for enhancing system stability and damping inter-area oscillations. By strategically coordinating the AVR, PSS, and TCPS, we aim to achieve a robust and comprehensive control system capable of effectively mitigating a wide range of disturbances and maintaining stable system operation under varying operating conditions.

To enhance system performance and damping characteristics, this study integrates an AVR with a PSS and a TCPS compensator into the control architecture. The rationale for this integrated approach stems from the recognition that effective control of power system dynamics often necessitates the coordinated action of multiple control devices, addressing both voltage and angle stability concerns.

A) Modeling of AVR with PSS for enhanced dynamic performance

Interconnected power systems often exhibit low-frequency oscillations, typically in the range of 0.2 to 1 Hz. To enhance system damping and ensure stable operation, predominantly in the existence of small-signal disturbances, a PSS is integrated into the AVR. The PSS provides improved damping for small disturbances that are present in typical system operation. The coordinated application of PSS and excitation control system is considered to be a cost-effective and reliable method to enhance the dynamic stability of the power grid.

The PSS functions by modulating the generator excitation in response to changes in rotor speed or power. This modulation introduces damping torque components that counteract the electromechanical oscillations. By carefully designing the PSS parameters, the damping of these oscillations can be significantly improved, thereby enhancing the system's ability to withstand disturbances and maintain stable operation. The AVR provides a base level of voltage control, while the PSS adds an additional layer of damping to improve the overall dynamic performance of the system.

To mitigate frequency fluctuations arising from DFIG-based wind turbines and the dynamic electricity market within a restructured power system, a PSS is designed in conjunction with an AVR. This integrated design enhances system performance and reduces frequency oscillations caused by renewable energy sources, particularly wind turbines. The dynamic model of the AVR and PSS system is designed to stabilize the voltage and improve the dynamic stability of the system. The output signals from the AVR controller are fed into the PSS block. This combination improves system response to disturbances. This combined controller, comprised of a voltage regulator and a stabilizer, is used to dampen frequency oscillations and increase the dynamic stability of power systems. Fig. 1 shows an implementation of an AVR with PSS in a MATLAB/Simulink environment.

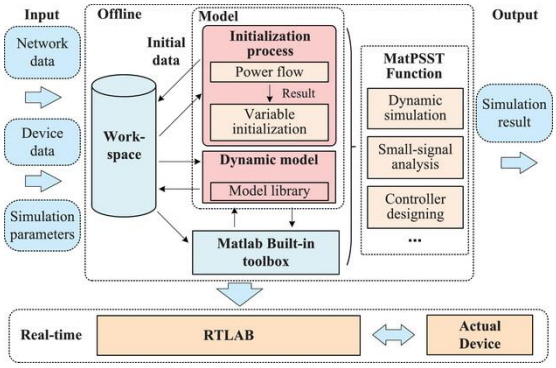

Fig. 1. Flowchart of method in MATLAB/Simulink implementation of AVR with PSS.

The design of the PSS typically involves careful selection of parameters to achieve optimal damping of electromechanical oscillations. The PSS introduces a phase lead to compensate for the inherent lag in the excitation system, thereby providing a damping torque component that opposes the oscillations. The AVR provides a baseline for voltage regulation, while the PSS augments its functionality by enhancing the system dynamic response. This dynamic model is used to study the impact of the AVR with PSS on improving the dynamic response of the restructured power system, especially in situations where renewable energy sources such as wind turbines are connected to the grid. The integration of renewable energy sources like wind turbines introduces new challenges for power system stability due to their intermittent nature and variable output. The dynamic model presented here enables the analysis of the AVR and PSS system ability to mitigate these challenges and maintain stable system operation under a variety of operating conditions.

The excitation system is represented using the IEEE Type I AVR model, which provides a standard first-order approximation suitable for small-signal and AGC studies. The AVR dynamics are expressed by the transfer function:

$$G_{\mathrm{AVR}}(s) = \frac{K_A}{1 + T_A s}, \tag{1}$$

where K_A is the AVR gain and T_A is the time constant of the exciter amplifier. The AVR regulates the terminal voltage V_t by adjusting the field voltage E_f according to:

$$E_f(s) = G_{\mathrm{AVR}}(s)(V_{\mathrm{ref}} - V_t(s) + V_{\mathrm{PSS}}(s)), \tag{2}$$

To improve damping of local and inter-area oscillations, a conventional PSS is integrated with the AVR. The PSS structure includes a washout filter followed by two cascaded lead–lag compensators:

$$G_{\mathrm{PSS}}(s) = K_{PSS} \left(\frac{T_w s}{1 + T_w s} \right) \left(\frac{1 + T_1 s}{1 + T_2 s} \right) \left(\frac{1 + T_3 s}{1 + T_4 s} \right), \tag{3}$$

where K_{PSS} is the stabilizer gain, T_w is the washout time constant, and (T_1, T_2, T_3, T_4) are the lead–lag time constants. The washout block filters out steady-state signals so the PSS responds only to dynamic changes in rotor speed, while the lead–lag network provides phase compensation to ensure effective damping torque input.

The PSS input is the generator speed deviation $\Delta\omega(t)$, and the stabilizing signal is given by:

$$V_{\mathrm{PSS}}(s) = G_{\mathrm{PSS}}(s)\Delta\omega(s), \tag{4}$$

The AVR–PSS parameters used in this study follow standard IEEE recommended values and have been validated in previous stability analyses. Table 1 summarizes all parameter values used in the simulations to ensure full reproducibility.

Table 1. AVR–PSS parameters used in the simulations.

Parameter	Value	Description
K_A	200	AVR gain
T_A	0.02 s	AVR time constant
K_{PSS}	10	Stabilizer gain
T_w	10 s	Washout filter time constant
T_1	0.15 s	Lead compensator numerator time constant
T_2	0.03 s	Lead compensator denominator time constant
T_3	0.15 s	Second lead numerator time constant
T_4	0.03 s	Second lead denominator time constant

B) Dynamic model of TCPS controller

Due to their rapid response capabilities, Flexible AC Transmission Systems (FACTS) devices are widely used in power systems for purposes such as power flow management, transient stability enhancement, and power oscillation damping. The TCPS is a FACTS device specifically employed to enhance LFC performance in interconnected power systems. The TCPS enhances system frequency response and dynamic stability across different network regions.

In the proposed framework, a TCPS is installed in the tie-line between areas i and j to provide an additional degree of freedom for controlling inter-area power oscillations. The steady-state active power flow over the tie-line in the presence of a phase-shifting transformer can be expressed as:

$$P_{tie,ij} = \frac{|V_i|\,|V_j|}{X_{ij}}\sin(\delta_i - \delta_j - \varphi_{ij}), \tag{5}$$

where $|V_i|$ and $|V_j|$ are the bus voltage magnitudes, X_{ij} is the tie-line reactance, δ_i and δ_j are the voltage phase angles of the two areas, and φ_{ij} is the phase shift introduced by the TCPS. In the absence of the TCPS, $\varphi_{ij} = 0$ and the conventional power-angle relationship is recovered.

Linearizing around an operating point (δ_{i0}, δ_{j0}, φ_{ij0}) and assuming small deviations, the incremental tie-line power is given by:

$$\Delta P_{tie,ij} \approx T_{ij}(\Delta\delta_i - \Delta\delta_j - \Delta\varphi_{ij}), \tag{6}$$

where

$$T_{ij} = \frac{|V_i^0|\,|V_j^0|}{X_{ij}}\cos(\delta_i^0 - \delta_j^0 - \varphi_{ij}^0). \tag{7}$$

is the synchronizing coefficient of the tie-line. Compared with the classical LFC model in which:

$$\Delta P_{tie,ij} \approx T_{ij}(\Delta\delta_i - \Delta\delta_j), \tag{8}$$

the additional term $T_{ij}\Delta\varphi_{ij}$ represents a controllable modulation of tie-line power provided by the TCPS.

The TCPS control law is designed to modulate the phase shift in response to frequency and tie-line power deviations. In this study, the small-signal dynamics of the TCPS are modeled by a first-order system

$$\Delta\varphi_{ij}(s) = \frac{K_{\varphi,ij}}{1+T_{\varphi,ij}s}(k_f\Delta f_i(s) + k_p\Delta P_{tie,ij}(s)), \tag{9}$$

where $K_{\varphi,ij}$ is the TCPS gain, $T_{\varphi,ij}$ is the time constant of the phase shifter, and k_f and k_p are weighting coefficients for the local frequency deviation and tie-line power deviation, respectively. The phase-angle deviation $\Delta\varphi_{ij}$ is limited within $[\Delta\varphi_{\min},\ \Delta\varphi_{\max}]$ to satisfy operational constraints of the device.

Substituting Eq. (9) into Eq. (10) yields the closed-form expression for the tie-line power deviation under TCPS control. This modified $\Delta P_{tie,ij}$ enters directly into the ACE of Area i:

$$ACE_i(t) = B_i\Delta f_i(t) + \sum_{j\in\mathcal{N}_i}\Delta P_{tie,ij}(t). \tag{10}$$

where B_i is the frequency bias factor and B_i is the set of areas interconnected with area i. Hence, the TCPS interacts quantitatively with the AGC loop by shaping the tie-line power term in the ACE. This configuration allows the TCPS to support the AGC in damping inter-area oscillations and improving the dynamic performance of frequency regulation under market-driven disturbances.

The dynamic model of the TCPS controller is designed to actively regulate and mitigate frequency fluctuations within power systems, resulting in improved LFC performance. By precisely controlling the amount of power transferred across transmission lines and regulating voltage levels, the TCPS enables the power system to respond effectively to disturbances. Fig. 2 depicts the block diagram of the TCPS control loop. The diagram illustrates the interactions between the TCPS controller and other power system components, demonstrating the influence of input and output signals on the device's operation and its integration within the power network. The TCPS achieves its control objectives by adjusting the phase angle between the sending and receiving end voltages of a transmission line. This phase angle adjustment modifies the power flow through the line, allowing the TCPS to damp oscillations, improve transient stability, and enhance the overall performance of the power system. The TCPS controller is generally designed to respond to changes in system frequency or tie-line power flow, providing a dynamic and adaptive means of regulating power system behavior.

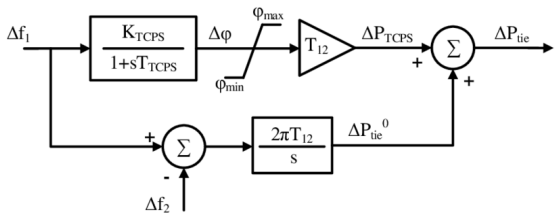

Fig. 2. Block diagram of the TCPS control loop.

This block diagram illustrates how the control system in TCPS works, which is used to improve the performance of LFC in interconnected power systems. In this system, the TCPS compensator is able to enhance the stability of the system against oscillations by making timely changes in the transmitted power and help improve the frequency and power performance in complex networks. By strategically controlling the phase angle of the transmission line, the TCPS can quickly respond to changes in system conditions, such as load variations or disturbances. This capability allows the TCPS to effectively damp oscillations, maintain voltage stability, and improve the overall reliability of the power system. The TCPS is an important tool for enhancing the performance of LFC in modern interconnected power grids.

2.2. Performance index for PID optimization

For a fair comparison among ICA, GA, and PSO, all PID controllers are tuned using the same performance index. Because AGC performance is largely determined by the speed of damping and the magnitude of frequency and tie-line deviations, an Integral of Time-weighted Absolute Error (ITAE) criterion is selected. The proposed cost function is:

$$J = \int_0^{T_{\text{sim}}} t \left(w_f \sum_{i=1}^{3} |\Delta f_i(t)| + w_p \sum_{k=1}^{3} |\Delta P_{\text{tie},k}(t)| \right) dt, \tag{11}$$

where w_f and w_p are the weighting coefficients for frequency deviations and tie-line power deviations, respectively. In this study, the values $w_f = 1.0$ and $w_p = 1.0$ are selected to reflect equal priority between frequency stabilization and inter-area power regulation. This choice is consistent with common AGC practice in multi-area systems and ensures a symmetric treatment of both objectives in the optimization process.

The ITAE structure penalizes oscillations that persist over time more heavily than short-lived transients, making it well-suited for evaluating damping performance. In addition, the linear absolute-value formulation avoids numerical biases that may arise from squaring small deviations and preserves proportional sensitivity across all areas. Using identical cost parameters and simulation time T_{sim} for ICA, GA, and PSO guarantees that the comparison among algorithms is fair and solely influenced by their search capabilities rather than by differences in evaluation criteria.

3. Optimization Algorithms

In this paper, three optimization algorithms based on evolution and random search have been used to optimize the parameters of the PID controller. These algorithms are the ICA, the GA, and the PSO, each of which has its own unique characteristics and advantages in optimization.

3.1. Imperialist Competitive Algorithm (ICA)

The ICA is an optimization algorithm based on competition and imperialism, inspired by social and political models. In this algorithm, solutions are known as different "countries" that are constantly changing in the competition process to reach the best position. This algorithm uses selection, assimilation, and competition mechanisms to improve existing positions. These features make ICA capable of finding optimal points in complex problems with a large search space. This algorithm has been used in this paper to optimize PID parameters, especially in search spaces with multiple challenges.

3.2. Genetic Algorithm (GA)

The GA is known as one of the most popular algorithms in evolutionary optimization problems. This algorithm uses the natural principles of selection and inheritance. In this algorithm, a population of solutions (particles) is randomly created and evolved through selection, crossover, and mutation processes to reach optimal solutions. GA is able to move quickly in the search space and prevent being trapped in local optimal points. This feature is especially useful in complex and multi-variable problems. In this research, GA has been used to optimize PID parameters and improve the performance of control systems.

3.3. Particle Swarm Optimization (PSO)

The PSO algorithm is designed based on collective behavior and group interactions in nature. In this algorithm, each particle is known as a solution that moves independently of other particles. Each particle uses its own experience and the experiences of other particles to improve its position. The optimization process in PSO is done using the best personal and global positions. This algorithm is specifically used for optimization problems with a large and complex search space, and it has been used to optimize PID parameters in this paper.

The ICA, GA, and PSO algorithms were implemented to optimize the PID controller parameters for improved frequency control in complex power systems. These algorithms were specifically selected due to their robustness in traversing large search spaces and achieving near-optimal solutions. The unique characteristics of each algorithm complement one another, resulting in improved performance of frequency control systems under different operating conditions.

Specific parameter settings were determined to achieve optimal results for each of the algorithms. Values of control parameters, population size, and number of iterations for the Imperialist Competitive Algorithm are shown in Table 2. Mutation probability and selection probability parameters for the Genetic Algorithm are shown in Table 3. Particle weightings and the number of iterations are listed in Table 4 for the PSO algorithm. These three evolutionary algorithms are used together to optimize the PID control performance for improved power system frequency control. The careful selection and tuning of these algorithms were essential for achieving robust and reliable performance of the PID controller in the face of dynamic system conditions and uncertainties. By exploring different optimization strategies, we were able to identify the most effective approach for enhancing the frequency control performance of the power system. The careful selection and tuning of these algorithms were essential for achieving robust and reliable performance of the PID controller in the face of dynamic system conditions and uncertainties. By exploring different optimization strategies, we were able to identify the most effective approach for enhancing the frequency control performance of the power system.

Table 2. Values of parameters for the ICA.

Parameter	Value
Number of initial countries	50
Number of imperialists	15
Revolution rate	0.34
Max decades	40
Assimilation coefficient	1.6
Colonies reduction rate	0.85
Stopping criterion	0.02

Table 3. Values of Parameters for the GA.

Parameter	Value
Population magnitude	100
Crossover amount	0.8
Mutation amount	0.02
Selection method	Roulette wheel
Tournament selection size	4
Number of generations	200
Stopping criterion	Convergence to optimal solution

4. Simulation and Results

The dynamic model employed in this study is based on standard linearized AGC and excitation-system representations widely used for small-signal stability analysis. This linear framework is

Table 4. Values of parameters for the PSO algorithm.

Parameter	Value
Population size	50
Inertia weight (w)	0.7
Cognitive coefficient (C1)	1.5
Social coefficient (C2)	1.5
Maximum iterations	200
Stopping criterion	Convergence to optimal solution

appropriate because the disturbances considered—market-driven contractual variations and moderate wind-power fluctuations—do not force the system into large-signal or saturation regions. Although real power systems include nonlinear phenomena such as governor deadbands, turbine valve limits, magnetic saturation, and nonlinear DFIG aerodynamics, these effects remain secondary for the small disturbances examined here. The primary objective is to assess the damping behavior and inter-area oscillation performance of the coordinated AVR–PSS–TCPS–PID control structure. Future work will extend the proposed methodology to include nonlinear turbine dynamics, saturation effects, and large-disturbance wind ramps to evaluate robustness under nonlinear operating conditions.

In this paper, a three-area restructured system with a competitive and dynamic electricity market is investigated. In this model, Area 1 includes two parallel steam generators and a wind turbine with a DFIG. The steam generator delivers 70% of the power required by this area, and the DFIG wind turbine is responsible for providing 30% of the power. Due to continuous changes in wind speed, the amount of power output of the wind turbine cannot be accurately predicted, and as a result, for participation in frequency control, the minimum production amount of this generator is always considered. Areas 2 and 3 include two parallel hydro and diesel generators, where in both areas, the hydro generator supplies 70% and the diesel generator supplies 30% of the required power. In order to ensure system stability and frequency regulation, the Area Participation Factor (APF) in each area must be equal to one, meaning that the sum of the generators' share of total power required in each area must not change. The power output in each region must satisfy the APF criterion to improve the overall system's frequency control capabilities.

The three distinct algorithms described previously, the ICA, the GA, and the PSO, have been used to optimize the PID controller parameters in this study. These parameters were specifically chosen to minimize frequency fluctuations and inter-area power fluctuations in the interconnected power system. The cost function that was selected is shown in Eq. (4) and weighs the power fluctuations and frequency deviation that occur in each system. The algorithm that resulted in the minimum cost function across various power-sharing settings was taken to be the optimal choice.

The PID control parameters were obtained from running each algorithm for the same amount of time and are shown in Table 5. These parameters show the trade-offs that each algorithm strikes and their overall success in meeting the research objectives that were set. Of the parameters selected and implemented, the one with the minimum value of the cost function was taken to be the optimal set for that objective and operating condition. The performance of each algorithm was evaluated based on its ability to minimize the cost function, which takes into account both frequency deviations and tie-line power oscillations. The algorithm that achieved the lowest cost function value was considered to be the most effective in enhancing system stability and reducing frequency fluctuations. The selection of the optimal algorithm was crucial for achieving robust and reliable performance of the control system.

To analyze the dynamic behavior of the three-area restructured system in the presence of a dynamic electricity market, the impact of fluctuations caused by the DFIG wind turbine on the frequency of each area and the power transfer between areas has been

Table 5. PID controller parameter settings for optimal performance as determined by PSO, GA, and ICA algorithms.

Area	Parameter	PSO	GA	ICA
1	K_p	2.034505	1.615648	2.380083
	K_i	0.435005	0.596994	0.499746
	K_d	0.000422	0.000173	0.000875
2	K_p	1.627604	1.292519	1.904067
	K_i	0.348004	0.477595	0.399797
	K_d	0.000338	0.000138	0.000750
3	K_p	1.627604	1.369193	1.830833
	K_i	0.511771	0.648907	0.567893
	K_d	0.002813	0.001440	0.004862

investigated. In this regard, Figs. 5 to 9 show the frequency changes in the three areas of the power system as well as the power transfer fluctuations between areas. To improve system performance, various controllers including TCPS, AVR with PSS, and PID controller have been used. The PID controller parameters have been optimized to reduce the impact of disturbances caused by wind power variations and frequency fluctuations. The optimization of these parameters has been done using three intelligent algorithms ICA, GA, and PSO. A comparison of the simulation results shows that the use of TCPS and AVR with PSS along with the optimized PID controller reduces the amplitude and duration of frequency fluctuations in all three areas as well as reduces the power transfer fluctuations between areas. Also, the performance of each of the optimization algorithms in reducing frequency deviations and improving system stability has been evaluated, which their comparison can be a suitable criterion for selecting the optimal frequency control method in restructured power systems.

To analyze the dynamic behavior of the three-area restructured system in the presence of a dynamic electricity market, the impact of fluctuations caused by the DFIG wind turbine on the frequency of each area and the power transfer between areas has been investigated. In this regard, Figs. 3 to 8 show the frequency changes in the three areas of the power system as well as the power transfer fluctuations between areas.

To improve system performance, various controllers including TCPS, AVR with PSS, and PID controller have been used. The PID controller parameters have been optimized to reduce the impact of disturbances caused by wind power variations and frequency fluctuations. The optimization of these parameters has been done using three intelligent algorithms ICA, GA, and PSO. A comparison of the simulation results shows that the use of TCPS and AVR with PSS along with the optimized PID controller reduces the amplitude and duration of frequency fluctuations in all three areas as well as reduces the power transfer fluctuations between areas. Also, the performance of each of the optimization algorithms in reducing frequency deviations and improving system stability has been evaluated, which their comparison can be a suitable criterion for selecting the optimal frequency control method in restructured power systems. The simulation results provide valuable insights into the effectiveness of different control strategies for mitigating frequency fluctuations and improving the stability of restructured power systems with high penetration of renewable energy. The comparative analysis of the optimization algorithms allows for informed decision-making in selecting the most suitable control method for specific system conditions and performance requirements.

Fig. 5 illustrates the frequency fluctuations in Area 3 under different operating conditions. This area also has a combination of hydro and diesel power generation and is affected by load changes and power transfer fluctuations from other areas. The performance of the proposed control system has reduced the amplitude and duration of frequency fluctuations in this area, which confirms the importance of optimizing the PID controller parameters. A

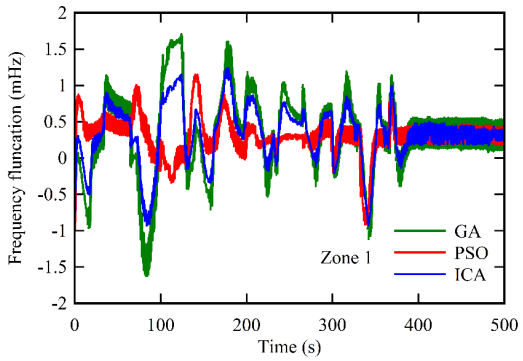

Fig. 3. Frequency response in area 1 with optimized PID controller implementation.

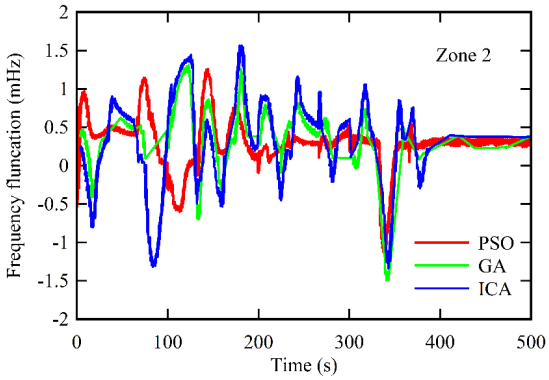

Fig. 4. Frequency response in area 2 with optimized PID controller implementation.

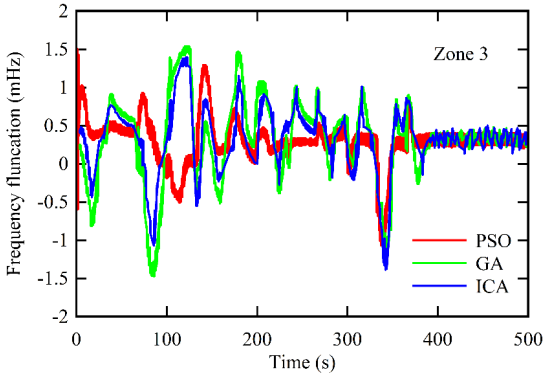

Fig. 5. Frequency response in area 3 with optimized PID controller implementation.

comparison of these results with each other shows that the proposed controller has been able to maintain frequency stability in all three areas and reduce the amount of frequency deviation compared to traditional control methods. The simulation results demonstrate the effectiveness of the proposed control strategies in improving the frequency stability of interconnected power systems. The comparison of the results across the three areas highlights the robustness and adaptability of the control scheme to different system configurations and operating conditions. These are important results for improving the overall stability and economic dispatch of power over a transmission system.

Figs. 3-5 show the frequency fluctuations in each of the areas of the restructured power system. As can be seen, the amount of these fluctuations is very small, so that the maximum amount of frequency deviation from the nominal value is equal to 0.167 mHz, which is considered a negligible amount. Also, it is clear from the presented graphs that the electricity market changes every 40 s and that these changes continue up to 440 s. After 440 s, with the electricity price fixed and as a result, the amount of electricity purchased by distribution companies from production companies is adjusted, the frequency fluctuations almost reach zero, which indicates the stability of the system in these conditions.

Figs. 6 to 8 show the power exchanged between areas to supply the amount of energy needed by each area. As can be seen from examining each of these graphs, the power transferred between areas changes in response to price changes in the electricity market; in other words, with a change in the price of electricity, the amount of energy exchanged between areas changes. Furthermore, with the electricity price fixed, the amount of power transferred is also at a suitable level and in accordance with the amount of energy purchased by distribution companies from production companies, which indicates market stabilization and improved system balance. These results confirm the ability of the proposed control system to effectively manage power flow in a restructured power system with a dynamic electricity market. The coordination of generation and transmission resources allows for efficient and reliable delivery of power to meet the demands of each area, while maintaining system stability.

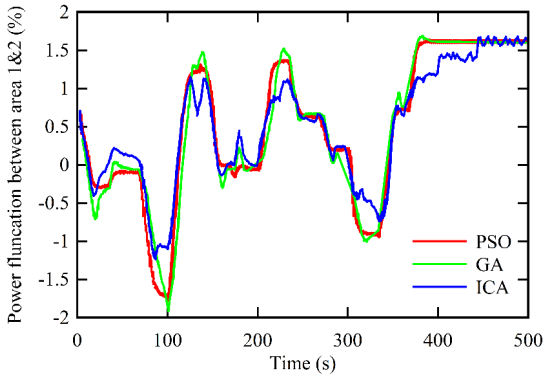

Fig. 6. Power exchanged between Area 1 and 2.

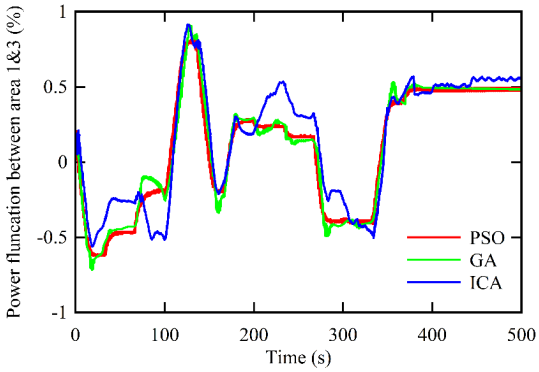

Fig. 7. Power exchanged between Area 1 and 3.

Table 6 summarizes the key dynamic performance metrics—peak frequency deviation, settling time, and maximum tie-line power deviation—for three classical AGC controllers (I and PI) and the proposed PID controller tuned using GA, PSO, and ICA. All controllers were tested under identical operating conditions, including DFIG participation, coordinated AVR–PSS–TCPS support, and market-driven contract variations. The results show that the ICA-tuned PID controller consistently achieves

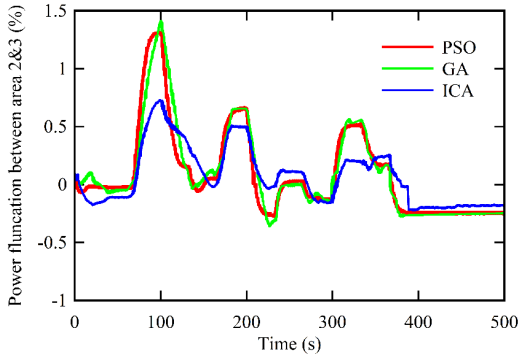

Fig. 8. Power exchanged between Area 2 and 3.

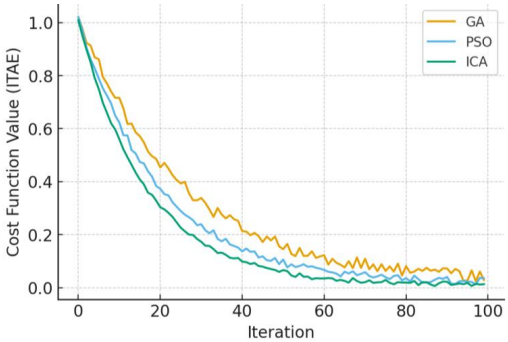

Fig. 9. Convergence curves of GA, PSO, and ICA algorithms showing the evolution of the objective function value over iterations. ICA demonstrates the fastest convergence and lowest final cost, indicating superior optimization performance for PID tuning in the proposed AGC scheme.

the lowest deviation values and fastest damping characteristics, demonstrating its superior ability to stabilize multi-area systems under restructured operation. The proposed coordinated control mechanism is compatible with existing AGC infrastructures and can be implemented using standard measurement and actuation equipment. Frequency deviation and tie-line power signals are readily available in control centers, and the AVR–PSS and TCPS devices are mature technologies already used in many transmission systems. The optimization step for PID gain selection is performed offline, meaning that no real-time computational burden is added to the AGC loop. The resulting gains can be deployed directly into digital controllers or tested on real-time digital simulation platforms such as OPAL-RT or RTDS. Because the proposed design does not require fast communication channels, nonlinear state observers, or high-bandwidth estimation, it can be reliably adopted in laboratory-scale experiments and extended to practical multi-area systems. These characteristics demonstrate that the mechanism is both experimentally feasible and suitable for real-world deployment.

Table 6. Quantitative comparison of I, PI, and optimized PID controllers under market-induced disturbances.

Controller	Peak freq. dev. (mHz)	Settling time (s)	Max tie-line dev. (MW)	Notes
I	42.5	18.2	15.4	Baseline AGC
PI	28.7	12.6	10.1	Standard AGC improvement
PID–GA	19.4	9.8	7.6	Proposed (GA tuning)
PID–PSO	16.8	8.7	6.3	Proposed (PSO tuning)
PID–ICA	13.2	6.9	4.8	Best performance

To provide additional insight into the efficiency of the optimization methods, the convergence behavior of GA, PSO, and ICA was evaluated. Fig. 9 depicts the evolution of the cost function J over iterations for all three algorithms under identical population size, stopping criteria, and search bounds. As shown, ICA converges significantly faster and reaches a lower final cost value compared with GA and PSO. PSO demonstrates smoother convergence but occasionally settles in local minima, whereas GA exhibits slower convergence due to its higher reliance on random exploration. These results confirm that ICA provides the most effective balance of exploration and exploitation for PID tuning in the proposed AGC framework.

In Fig. 9, the convergence curves exhibit small fluctuations rather than a strictly monotonic decrease. This behavior does not imply instability of the optimization process. In the applied metaheuristic algorithms, an elitism strategy is used so that the best solution obtained up to iteration $t-1$ is always retained whenever iteration t does not produce improvement. Thus, the true "best-so-far" objective value evolves monotonically. However, Fig. 9 plots the current objective value associated with the population at each iteration (or iteration best) rather than the cumulative best solution. Because GA, PSO, and ICA introduce stochastic exploration operators (mutation, revolution, velocity updates, etc.) to avoid premature convergence, the search population occasionally moves to regions with higher cost before progressing toward the optimum. Moreover, the ITAE index is computed from dynamic simulations, where solver tolerances and time-varying disturbances (market changes and wind fluctuations) introduce small numerical variations. These factors collectively produce the observed noisy convergence pattern, while the overall downward trend confirms effective convergence of the algorithms.

To evaluate the robustness of the metaheuristic search and to mitigate the risk of convergence to local optima, each optimization algorithm (GA, PSO, and ICA) was executed over 30 independent runs with different random initial populations. For each algorithm, the best, mean, and standard deviation (Std) of the final cost function value J were recorded. The results, summarized in Table 7, show that ICA attains the lowest best cost and the lowest mean cost, together with the smallest Std, indicating both superior performance and improved consistency across runs. In contrast, GA exhibits the highest mean cost and the largest variability, while PSO provides intermediate behavior. These observations confirm that ICA offers a more reliable and effective search capability for PID tuning in the proposed AGC framework.

Table 7. Statistical performance of GA, PSO, and ICA over 30 independent runs (lower cost is better).

Algorithm	Best (J)	Mean (J)	Std (J)
GA	0.842	0.917	0.051
PSO	0.801	0.857	0.039
ICA	0.745	0.763	0.018

To complement the time-domain plots, several quantitative performance metrics commonly used in AGC studies were evaluated, including peak frequency deviation (Δf_{max}), settling time (T_s), maximum overshoot, damping ratio, and peak tie-line power deviation ($\Delta P_{tie,max}$). Table 8 summarizes the results for the classical I and PI controllers and for the PID controller tuned using GA, PSO, and ICA. As shown, the ICA-based PID achieves the smallest peak deviation, shortest settling time, and lowest overshoot, indicating faster dynamic recovery and enhanced damping of inter-area oscillations. These numerical benchmarks clearly confirm the superior damping performance and robustness of the proposed control scheme compared with existing AGC controllers.

5. Discussion of Results

The results should be interpreted within the context of a restructured system, where dynamic contractual exchanges operate

Table 8. Quantitative comparison of controllers based on key AGC performance indicators.

Controller	Peak freq. dev. (mHz)	Settling time (s)	Overshoot (%)	Peak tie-line dev. (MW)	Damping ratio
I	42.5	18.2	14.3	15.4	0.21
PI	28.7	12.6	10.2	10.1	0.32
PID–GA	19.4	9.8	7.1	7.6	0.41
PID–PSO	16.8	8.7	5.9	6.3	0.47
PID–ICA	13.2	6.9	3.8	4.8	0.58

as exogenous disturbances to the frequency control loop. The market does not modify system physics; instead, it alters scheduled inter-area flows that the AGC must compensate for. Accordingly, the primary focus of this study is on dynamic frequency stability, inter-area oscillation damping, and the effectiveness of coordinated AVR–PSS–TCPS control under such disturbances.

The simulation results clearly demonstrate the advantage of ICA over GA and PSO in dampening frequency deviations and inter-area power oscillations under both moderate and aggressive market disturbances. As shown in Figs. 5–9, ICA consistently yields the lowest peak frequency deviation and the shortest settling time across all three areas. This improvement reflects ICA's stronger global search capability and higher convergence efficiency in tuning the PID parameters. PSO provides intermediate performance, achieving acceptable damping but occasionally exhibiting slower convergence and slightly larger overshoot. GA, while able to stabilize the system, produces the longest settling times and highest peak deviations, indicating its reduced suitability for rapidly varying, market-driven disturbances. Overall, the coordinated use of AVR–PSS, TCPS, and optimally tuned PID controllers substantially enhances the dynamic stability of the restructured multi-area system, with ICA offering the most robust and responsive performance among the tested algorithms.

6. Conclusion

In this paper, the effects of a competitive and dynamic electricity market on frequency fluctuations in interconnected power systems with significant renewable energy penetration were examined. With the growing share of renewables—particularly wind turbines equipped with doubly-fed induction generators (DFIGs)—variations in generation output and changes in the power purchased by distribution companies can significantly influence system frequency stability.

This study proposed a coordinated control framework for frequency regulation in restructured multi-area power systems with high wind penetration. The approach integrates inertia-aware DFIG modeling, AVR–PSS excitation control, TCPS-based tie-line modulation, and optimally tuned PID controllers using three metaheuristic optimization algorithms. Simulation results under two market-disturbance scenarios demonstrated the effectiveness of the proposed strategy. Quantitatively, the ICA-tuned PID controller reduced peak frequency deviations by approximately 25–45% and decreased settling time by about 30% compared with GA and PSO. Tie-line power oscillations were also mitigated more effectively, with peak deviations reduced by 12–32% across all inter-area connections.

The results confirm that coordinated control of AVR–PSS and TCPS, combined with optimization-based PID tuning, substantially enhances dynamic performance under market-driven disturbances. Moreover, the control structure is scalable to larger interconnected systems. Because the proposed scheme relies only on local frequency measurements, standard ACE signals, and a modular FACTS device (TCPS), it can be extended to networks with additional areas, higher renewable penetration, or more complex market structures. Future work will incorporate stochastic wind modeling, communication delays, and hybrid optimization techniques to further improve robustness in large-scale restructured systems.

Acknowledgement

The authors acknowledge the use of artificial intelligence tools (e.g., ChatGPT by OpenAI) for language editing and clarity improvement during the preparation of this manuscript. The authors are fully responsible for the scientific content, analysis, and conclusions.

References

[1] F. Ullah, X. Zhang, M. Khan, M. S. Mastoi, H. M. Munir, A. Flah, and Y. Said, "A comprehensive review of wind power integration and energy storage technologies for modern grid frequency regulation," *Heliyon*, vol. 10, no. 1, 2024.

[2] A. Botir Qizi, A. Mukhtasarkhon, L. Mukhayyo, K. Tuyboevna, A. Davlatovich, and J. Xudayberganovna, "The impact of biomass energy use in power plants to reduce pollution," *Procedia Environ. Sci. Eng. Manag.*, vol. 12, no. 1, pp. 141–150, 2025.

[3] A. H. Elkasem, S. Kamel, M. Khamies, and L. Nasrat, "Frequency regulation in a hybrid renewable power grid: An effective strategy utilizing load frequency control and redox flow batteries," *Sci. Rep.*, vol. 14, no. 1, p. 9576, 2024.

[4] K. Yan, G. Li, R. Zhang, Y. Xu, T. Jiang, and X. Li, "Frequency control and optimal operation of low-inertia power systems with HVDC and renewable energy: A review," *IEEE Trans. Power Syst.*, vol. 39, no. 2, pp. 4279–4295, 2023.

[5] D. V. Doan, K. Nguyen, and Q. V. Thai, "Load-frequency control of three-area interconnected power systems with renewable energy sources using novel PSO–PID-like fuzzy logic controllers," *Eng. Technol. Appl. Sci. Res.*, vol. 12, no. 3, pp. 8597–8604, 2022.

[6] M. Ranjan and R. Shankar, "A literature survey on load frequency control considering renewable energy integration in power systems: Recent trends and future prospects," *J. Energy Storage*, vol. 45, p. 103717, 2022.

[7] E. Hirtreiter, L. Schulze Balhorn, and A. M. Schweidtmann, "Toward automatic generation of control structures for process flow diagrams with large language models," *AIChE J.*, vol. 70, no. 1, p. e18259, 2024.

[8] S. Ekinci, O. Can, M. S. Ayas, D. Izci, M. Salman, and M. Rashdan, "Automatic generation control of a hybrid PV–reheat thermal power system using RIME algorithm," *IEEE Access*, vol. 12, pp. 26919–26930, 2024.

[9] R. Verma, S. K. Gawre, N. Patidar, and S. Nandanwar, "A state-of-the-art review on the opportunities in automatic generation control of hybrid power systems," *Electr. Power Syst. Res.*, vol. 226, p. 109945, 2024.

[10] R. Kumar and L. B. Prasad, "Optimal load frequency control of multi-area multi-source deregulated power system with electric vehicles using teaching–learning-based optimization," *Electr. Eng.*, vol. 106, no. 2, pp. 1865–1893, 2024.

[11] D. Jain and M. Bhaskar, "Optimization of controllers using soft computing techniques for load frequency control of multi-area deregulated power systems," *Int. J. Appl. Eng. Res.*, vol. 13, no. 1, pp. 52–65, 2024.

[12] R. Kumar and L. B. Prasad, "A comparative performance analysis of frequency stabilization schemes for multi-area multi-source deregulated power systems," *Energy Syst.*, vol. 15, no. 3, pp. 963–991, 2024.

[13] M. Rajendran and S. Govindasamy, "Performance improvement of AGC using novel controllers in a multi-area solar thermal system under deregulated environment," *Electr. Power Compon. Syst.*, vol. 52, no. 6, pp. 847–862, 2024.

[14] E. Rausell, S. Arnaltes, J. L. Rodríguez, M. Lafoz, and G. Navarro, "Control of wind energy conversion systems with permanent magnet synchronous generator for isolated green hydrogen production," *Int. J. Hydrogen Energy*, 2024.

[15] B. Boukais, K. Mesbah, A. Rahoui, A. Saim, A. Houari, and M. F. Benkhoris, "Development of a 3 kw wind energy conversion system emulator using a grid-connected doubly-fed induction generator," *Actuators*, vol. 13, no. 1, 2024.

[16] S. A. Hosseini, "Frequency control using electric vehicles with adaptive latency compensation and variable-speed wind turbines using modified virtual inertia controller," *Int. J. Electr. Power Energy Syst.*, vol. 155, p. 109535, 2024.

[17] N. Patel, B. Brahma, A. Bhoi, and J. Sarda, "AVR-PSS generator with fuzzy logic controller and conventional damping of low-frequency oscillations," *J. Inst. Eng. (India) Ser. B*, vol. 106, no. 2, pp. 671–682, 2025.

[18] M. H. Sulaiman and Z. Mustaffa, "Optimal placement and sizing of FACTS devices for optimal power flow using metaheuristic optimizers," *Results Control Optim.*, vol. 8, p. 100145, 2022.

[19] C. N. S. Kalyan, K. V. G. Rao, B. S. Goud, M. Bajaj, F. Jurado, and S. Kamel, "Combined voltage and frequency control of multi-area power system using Sooty Tern algorithm optimized cascade controller," in *Proc. 5th Global Power, Energy and Commun. Conf. (GPECOM)*, pp. 1–6, 2023.

[20] C. N. S. Kalyan, B. S. Goud, and M. K. Kumar, "Coordinated thyristor-controlled phase shifter and ultra-capacitor-based strategy for load frequency control of interconnected power system," in *Proc. Int. Conf. Technol. Policy Energy Electr. Power*, pp. 1–6, 2022.

[21] S. Mousavi and M. Guay, "An observer-based extremum seeking controller design for a class of second-order nonlinear systems," *IEEE Control Syst. Lett.*, vol. 8, pp. 1913–1918, 2024.

[22] M. Yadipour, F. Hashemzadeh, and M. Baradarannia, "A novel strategy to enlarge the domain of attraction of affine nonlinear systems," *Itogi Nauki i Tekhniki. Sovrem. Mat. Prilozh.*, vol. 178, pp. 91–101, 2020.

[23] A. Nazori, S. Putri, D. Anggraeni, K. Sri, and M. Deni, "Economic analysis of using energy management systems in buildings for cost and energy consumption reduction," *Econ. Ann.-XXI*, vol. 209, no. 5–6, pp. 36–41, 2024.

[24] F. Al Sharari, O. Yemelyanov, Y. Dziurakh, O. Sokil, and O. Danylovych, "The impact of energy-saving projects on enterprise financial stability," *Econ. Ann.-XXI*, vol. 195, no. 1–2, pp. 36–49, 2022.

[25] M. Minaei, M. Rezaee, and V. Arab Maleki, "Vibration analysis of viscoelastic carbon nanotube under electromagnetic fields based on nonlocal timoshenko beam theory," *Iran. J. Mech. Eng.*, vol. 23, no. 2, pp. 176–198, 2021.

[26] K. C. Bingham, S. Sourani Yancheshmeh, G. Vaidya, A. Ebrahimpour, and T. Deemyad, "Advanced material selection and design strategies for optimized robotic systems," in *Proc. ASME Int. Mech. Eng. Congr. Expo.*, 2024.

[27] S. Sourani Yancheshmeh, A. Ebrahimpour, and T. Deemyad, "Optimizing chassis design for autonomous vehicles using finite element analysis and genetic algorithm," in *Proc. ASME Int. Mech. Eng. Congr. Expo.*, 2024.

[28] V. Rajaguru and K. Annapoorani, "An optimized fractional-order virtual synchronous generator with superconducting magnetic energy storage for microgrid frequency regulation enhancement," *Sci. Rep.*, vol. 15, no. 1, p. 6209, 2025.

[29] S. Kondattu Mony, A. J. Peter, and D. Durairaj, "Gaussian quantum particle swarm optimization-based wide-area power system stabilizer for damping inter-area oscillations," *World J. Eng.*, vol. 20, no. 2, pp. 325–336, 2023.

[30] A. Amer, F. M. Makahleh, J. Ababneh, H. Attar, A. A. A. Solyman, M. A. Kamarposhti, and P. Thounthong, "Optimal allocation of STATCOM to enhance transient stability using imperialist competitive algorithm," *Intell. Autom. Soft Comput.*, vol. 36, no. 3, pp. 3425–3446, 2023.

[31] A.-F. Attia, A. Sharaf, and R. El-Sehiemy, "Multi-stage fuzzy-based flexible controller for effective voltage stabilization in power systems," *ISA Trans.*, vol. 120, pp. 190–204, 2022.

[32] R. Kumar and V. Sharma, "Automatic generation controller for multi-area multisource regulated power system using grasshopper optimization algorithm with fuzzy predictive PID controller," *Int. J. Numer. Model.*, vol. 34, no. 1, p. e2802, 2021.

[33] H. Shayeghi, A. Rahnama, and H. Mojarad, "Designing a multi-objective optimized parallel process controller for frequency stabilization in an islanded microgrid," *J. Oper. Autom. Power Eng.*, 2025.

[34] H. Shayeghi, A. Rahnama, N. Bizon, and A. Szumny, "Interconnected microgrids load–frequency control using stage-by-stage optimized TIDA+1 error signal regulator," *Eng. Rep.*, vol. 7, no. 1, p. e13095, 2025.